



OPEN

Multiplex quantification of C-terminal alpha-1-antitrypsin peptides provides a novel approach for characterizing systemic inflammation

Arite Bigalke¹, Christoph Sponholz², Claudia Schnabel¹, Michael Bauer² & Michael Kiehntopf¹

C-terminal peptides (CAAPs) of the highly abundant serine protease alpha-1-antitrypsin (A1AT) have been identified at various lengths in several human materials and have been proposed to serve as putative biomarkers for a variety of diseases. CAAPs are enzymatically formed and these enzymatic activities are often associated with excessive immune responses (e.g. sepsis, allergies). However, most of those CAAPs have been either detected using in vitro incubation experiments or in human materials which are not easily accessible. To gain a comprehensive understanding about the occurrence and function of CAAPs in health and disease, a LC-MS/MS method for the simultaneous detection of nine CAAPs was developed and validated for human plasma (EDTA and lithium-heparin) and serum. Using this newly developed method, we were able to detect and quantify five CAAPs in healthy individuals thereby providing an initial proof for the presence of C36, C37, C40 and C44 in human blood. Concentrations of four CAAPs in a clinical test cohort of patients suffering from sepsis were significantly higher compared to healthy controls. These results reveal that in addition to C42 other fragments of A1AT seem to play a crucial role during systemic infections. The proposed workflow is simple, rapid and robust; thus this method could be used as diagnostic tool in routine clinical chemistry as well as for research applications for elucidating the diagnostic potential of CAAPs in numerous diseases. To this end, we also provide an overview about the current state of knowledge for CAAPs identified in vitro and in vivo.

The endogenous balance between inhibitory active forms of the major human SERPIN alpha-1-antitrypsin (A1AT) and its target-proteinases (primarily human neutrophil elastase, HNE) is a crucial factor determining whether local inflammation processes will result in larger connective tissue damage^{1–3}. Complex formation of A1AT with serine proteases does not only cause inactivation of both substrates but also cleavage of the SERPIN at the reactive site centered at Met³⁸²-Ser. However, several non-target enzymes are also able to cleave A1AT in the RCL (reactive center loop) region causing functional loss of the primary regulator towards human serine proteinases and thus increase the risk for the development of lung emphysema and other acute or chronic inflammatory conditions which are known pathophysiological consequences among A1AT deficient individuals⁴.

During the process of A1AT cleavage by certain enzymes (with or without complex formation), carboxyl-terminal peptides of A1AT (CAAPs) of various lengths can emerge. In addition to HNE which provokes the formation of C36 when complexed to A1AT⁵, many other enzymes have been identified exhibiting efficient A1AT degradation activity with simultaneous generation of CAAPs. Those enzymes include either endogenous human proteases (mainly matrix-metalloproteinases)^{5–25}, proteases found in microbes causing infections^{26–32} or proteases that act as allergens for human allergic disorders^{33–35}. However, CAAPs have been detected predominantly by using in vitro incubation experiments with purified A1AT. A few CAAPs have also been identified in vivo in human tissue and liquids such as urine³⁶, bronchoalveolar lavage fluid^{37,38}, gingival crevicular fluid³⁹, spleen and

¹Department of Clinical Chemistry and Laboratory Medicine, Jena University Hospital, Jena, Germany. ²Department of Anesthesiology and Intensive Care Therapy, Jena University Hospital, Jena, Germany. ✉ email: arite.bigalke@gmail.com; michael.kiehntopf@med.uni-jena.de

bile⁴⁰, lung tissue⁴¹, carotid artery tissue⁴², placenta^{43,44} and nipple aspiration fluids⁴⁵. Some CAAPs were proposed to serve as putative biomarkers for glomerular kidney diseases³⁶, pulmonary fibrosis³⁸, gingivitis³⁹ and carotid artery stenosis⁴². However, C42 (“CAAP48/47”) is the hitherto only CAAP detected in human blood⁴⁶. In this previous study, C42 has been shown to function as inflammatory marker because C42 levels were significantly elevated in patients with severe sepsis compared with patients with systemic inflammatory response syndrome (SIRS) or HIV, respectively. Due to the higher concentrations of C42 found in the sepsis compared to SIRS group, a crucial role of microbes frequently triggering septic shock can be assumed. This is supported by the fact that extracellular microbial proteases, identified *in vitro* as CAAP-generating enzymes, serve as virulence factors for *Staphylococcus aureus*^{27–29}, *Pseudomonas aeruginosa*^{27,30}, *Serratia marcescens*^{27,31} and *Candida albicans*⁴⁷. In addition to the role of C42 as sepsis biomarker, CAAPs reveal immunomodulatory functions as well and thus might contribute themselves to the inflammatory process. Among the multiplicity of A1AT cleavage fragments, C36 and C42 are the best studied CAAPs regarding their inflammatory immune modulating functions. They act, for example, as chemoattractant for phagocytes and monocytes⁴⁸, activators of human monocytes and neutrophils *in vitro*^{41,42,46,49}, neutrophil extracellular trap inhibitory substances⁵⁰ and alter hepatic functions and gene expression *in vitro* and *in vivo*^{51,52}. From a pathophysiological perspective, CAAPs seem to be highly relevant as diagnostic tools for the identification of a variety of diseases. However, the diagnostic use of CAAP profiles is still associated with some challenges. First, CAAPs are likely not equally distributed among the human body. Second, many enzymes are capable to cleave A1AT at more than only one position in the RCL region. Third, knowledge gained from *in vitro* experiments cannot directly translated to natural and therefore more complex environments such as the human body.

To better understand the complexity of mechanisms leading to CAAP formation, we focused on the development of a diagnostic tool determining CAAP patterns. To this end, we implemented a fast, multiplexed LC–MS/MS method for the simultaneous quantification of nine CAAPs in human serum and plasma; readily available and widely-used biomaterial.

Results

A variety of cleavage products of the major plasma protease inhibitor alpha-1-antitrypsin (CAAPs) have been observed *in vitro* by incubation of alpha-1-antitrypsin with proteases as well as *in vivo* in several human tissues. With the exception of C42 (“CAAP48/47”) ⁴⁶, none of those CAAPs have been detected in human blood yet. Due to the vital role of CAAPs during inflammatory infection and possibly other diseases, a rapid method using readily available biomaterials such as blood-derived specimens is needed. Therefore, nine full-length C-terminal peptides were selected and synthesized compromising each CAAP amino acid lengths (from C45 to C22) in WT (wild type) and SNP (single nucleotide polymorphism) variant rs1303⁵³, respectively. In order to be able to quantitatively measure this peptide panel a multiplex MRM-based method was established and validated^{54,55} for human plasma (EDTA and lithium-heparin) and serum.

Method validation

Linearity, working range, carry-over and specificity. Nine calibrants were used in total ranging from 0.01 μM to 1.5 μM thereby covering more than two orders of magnitude in concentration. In eight independent analytical runs, mean coefficients of determination of each calibration curve from 0.01 to 1.5 μM were $R^2 \geq 0.996$ for each compound (CV < 0.4%, n = 8, respectively) except for C43^{WT} and C43^{SNP} which were $R^2 \geq 0.992$ (CV \leq 0.31%, n = 8, respectively). These results demonstrate sufficient *linearity* throughout the entire calibration range. Working ranges for each of the CAAPs were set according to concentrations in healthy and critically ill patients and were optimized during validation procedure (Table 1).

Carry-over was less than 5% of peak areas compared to respective LLOQ samples for all CAAPs and are thus in line with official recommendations (below 20% for analytes, Table 1)⁵⁵. In none of the blank albumin samples measured directly after respective ULOQ samples internal standards were detected.

No interferences (test of *specificity*) above the LLOQ were detected (Additional file 2). We detected a few WT-variants above 20% of the LLOQ in the presence of respective SNP-variants. There was further no interference greater than 5% between CAAPs and internal standard detection (Additional file 2).

Accuracy and precision. Mean accuracies and precisions (within-run repeatability and between-run) were within recommended ranges (maximum \pm 15% and \pm 20% for LLOQ, respectively) (Table 2).

Selectivity and investigation of matrix effects. Selectivity was determined in blank albumin samples and results revealed that no peaks (analyte or internal standards) were detected. Serial dilutions of CAAPs standard in pool (human) matrices verified that the responses of concentrations in albumin, serum and plasma (EDTA and lithium-heparin) are linear, respectively (Additional file 3). Due to the unavailability of analyte-free biological matrix, matrix effects were investigated by determining recovery rates and precisions of each compound in different human whole blood derived specimens which were compared to zero albumin samples with equal amount of CAAPs added (using area ratios instead of back-calculated concentrations). Most of the analytes spiked into EDTA plasma were within \pm 20% of recovery compared to zero albumin sample (Table 3). Precisions were \leq 10% between six individually analyzed human donors suggesting that matrix effects are low in EDTA plasma. Recovery rates of CAAPs in lithium-heparin as well as in serum were clearly lower than those in EDTA plasma revealing that effects of these matrices are considerably high. However, most of the CAAP concentrations in serum were consistently back-calculated among the six measured healthy individuals (precision \leq 20%).

Analyte	Working range (no. of calibrants)	Concentrations of QCs used for validation	Carry-over
C36 ^{WT}	0.025–1.5 μM (8)	QC2 (0.025 μM, LLOQ)/ QC3 (0.3 μM)/ QC4 (0.9 μM)	4%
C36 ^{SNP}			2%
C42 ^{WT}			2%
C42 ^{SNP}			1%
C37 ^{WT}	0.01–1 μM (8)	QC1 (0.01 μM, LLOQ) QC3 (0.3 μM) QC4 (0.9 μM)	0%
C37 ^{SNP}			0%
C22 ^{WT}	0.01–0.5 μM (7)	QC1 (0.01 μM, LLOQ) QC2 (0.025 μM) QC3 (0.3 μM)	0%
C22 ^{SNP}			1%
C39 ^{WT}			0%
C39 ^{SNP}			0%
C40 ^{WT}			0%
C43 ^{WT}			0%
C43 ^{SNP}			2%
C44 ^{WT}			0%
C44 ^{SNP}			2%
C45 ^{WT}			0%
C45 ^{SNP}			0%
C40 ^{SNP}			0.0036–0.1785 μM (7)

Table 1. Working ranges, QC sample concentrations and results of carry-over experiments. Carry-over is determined as the ratio of peak areas measured in blank albumin sample to peak areas of respective LLOQs (%).

Analyte	Quality control	Within-run repeatability (technical replicates, n = 5)		Between-run (independent runs, n = 5)	
		Accuracy (mean, %)	Precision (mean CV, %)	Accuracy (mean, %)	Precision (mean CV, %)
C36 ^{WT}	QC2/ QC3/ QC4	110/ 111/ 107	5/ 2/ 1	113/ 108/ 106	2/ 3/ 2
C36 ^{SNP}		113/ 108/ 104	1/ 3/ 1	113/ 107/ 104	1/ 2/ 2
C42 ^{WT}		109/ 107/ 104	2/ 2/ 3	110/ 106/ 105	3/ 2/ 3
C42 ^{SNP}		107/ 106/ 104	3/ 2/ 3	109/ 106/ 105	2/ 2/ 3
C37 ^{WT}	QC1/ QC3/ QC4	117/ 108/ 104	4/ 2/ 2	121/ 108/ 104	6/ 3/ 2
C37 ^{SNP}		113/ 107/ 105	5/ 2/ 3	117/ 105/ 103	2/ 2/ 3
C22 ^{WT}	QC1/ QC2/ QC3	99/ 100/ 100	2/ 3/ 3	103/ 105/ 102	4/ 4/ 2
C22 ^{SNP}		98/ 101/ 102	3/ 2/ 4	101/ 105/ 102	7/ 3/ 3
C39 ^{WT}		120/ 114/ 109	5/ 1/ 1	117/ 119/ 106	2/ 4/ 4
C39 ^{SNP}		111/ 111/ 103	3/ 4/ 2	117/ 110/ 103	7/ 3/ 1
C40 ^{WT}		115/ 112/ 106	3/ 4/ 2	117/ 112/ 106	2/ 3/ 2
C40 ^{SNP}		112/ 108/ 104	8/ 6/ 2	105/ 103/ 101	5/ 2/ 2
C43 ^{WT}		110/ 108/ 99	3/ 2/ 2	117/ 111/ 101	4/ 4/ 2
C43 ^{SNP}		109/ 107/ 100	5/ 2/ 2	117/ 112/ 103	5/ 3/ 3
C44 ^{WT}		117/ 113/ 103	1/ 2/ 2	118/ 112/ 103	10/ 7/ 4
C44 ^{SNP}		112/ 107/ 103	2/ 2/ 2	113/ 111/ 102	9/ 9/ 4
C45 ^{WT}		117/ 116/ 104	2/ 2/ 2	115/ 111/ 104	8/ 8/ 4
C45 ^{SNP}		112/ 111/ 102	5/ 1/ 2	111/ 111/ 102	6/ 5/ 4

Table 2. Accuracy and precision of repeated measurements.

To clarify reasons for high variations of peak area ratios of CAAPs in lithium-heparin plasma, variations of internal standards were additionally analyzed (Table 4).

High variations in recovery of CAAPs in lithium-heparin plasma derived most likely from inconsistent responses of all three internal standards in lithium-heparin plasma.

	EDTA plasma				Lithium-heparin plasma				Serum			
	Accuracy (mean, n = 6)		Precision (n = 6)		Accuracy (mean, n = 6)		Precision (n = 6)		Accuracy (mean, n = 6)		Precision (n = 6)	
	H	L	H	L	H	L	H	L	H	L	H	L
C22 ^{WT}	98%	99%	4%	1%	46%	46%	10%	13%	58%	59%	8%	13%
C22 ^{SNP}	98%	99%	3%	2%	46%	46%	11%	13%	58%	59%	8%	14%
C36 ^{WT}	99%	91%	2%	5%	25%	20%	21%	68%	49%	50%	10%	18%
C36 ^{SNP}	105%	109%	4%	4%	28%	29%	24%	38%	52%	53%	12%	14%
C37 ^{WT}	125%	126%	5%	6%	40%	42%	14%	14%	66%	65%	5%	9%
C37 ^{SNP}	129%	132%	4%	3%	51%	55%	11%	17%	80%	80%	6%	9%
C39 ^{WT}	84%	78%	6%	8%	31%	33%	16%	21%	47%	44%	11%	17%
C39 ^{SNP}	83%	80%	9%	10%	19%	21%	25%	30%	30%	29%	21%	27%
C40 ^{WT}	117%	105%	5%	8%	28%	28%	19%	22%	47%	43%	12%	14%
C40 ^{SNP}	102%	102%	5%	2%	27%	29%	17%	21%	43%	44%	13%	17%
C42 ^{WT}	100%	97%	2%	7%	36%	34%	13%	31%	52%	52%	9%	17%
C42 ^{SNP}	99%	103%	4%	7%	28%	28%	21%	31%	39%	39%	17%	21%
C43 ^{WT}	119%	121%	5%	6%	44%	45%	12%	13%	57%	55%	5%	7%
C43 ^{SNP}	113%	116%	3%	6%	33%	34%	14%	15%	38%	40%	11%	12%
C44 ^{WT}	81%	79%	8%	5%	18%	18%	19%	28%	25%	23%	11%	20%
C44 ^{SNP}	82%	80%	8%	6%	15%	17%	25%	39%	21%	22%	15%	23%
C45 ^{WT}	77%	72%	7%	10%	24%	20%	19%	23%	35%	27%	7%	14%
C45 ^{SNP}	88%	88%	8%	5%	20%	24%	21%	22%	30%	30%	12%	16%

Table 3. Recovery rates of spiked CAAP concentrations in different biological matrices. Accuracies and precisions are shown as mean of six voluntary donors. H: high CAAPs concentration; L: low CAAPs concentration.

	No. of values	Peak Area					
		C42 ^{IS}		C37 ^{IS}		C22 ^{IS}	
		mean	CV (%)	mean	CV (%)	mean	CV (%)
Albumin (H, L)	n = 4	9.2*10 ⁶	2.7%	7.0*10 ⁶	3.0%	7.9*10 ⁶	1.2%
EDTA (0, H, L)	n = 34	7.7*10 ⁶	6.4%	5.7*10 ⁶	9.6%	7.6*10 ⁶	5.4%
Li-Hep (0, H, L)	n = 35	6.7*10 ⁶	18.5%	4.7*10 ⁶	19.4%	7.3*10 ⁶	14.1%
Serum (0, H, L)	n = 33	6.0*10 ⁶	8.5%	4.2*10 ⁶	10.2%	7.0*10 ⁶	6.4%

Table 4. Mean peak areas and precisions of internal standards in different biological matrices. Different CAAP concentrations were spiked into each of the individual matrices: 0 = pure albumin; H: high CAAPs concentration; L: low CAAPs concentration.

Stability. Stability of analytes in processed samples was determined at six independent days for a time span of 20 h in the autosampler. Deviations of standing samples to freshly measured samples were below 19% at the LLOQ and below 9% for other QC levels for each analyte, respectively (Additional file 4). Stability of analytes in biological matrix was determined by consecutive cycles of freezing and thawing as well as extended intervals at room temperature from thawing to processing (approximately one hour). Deviations of either freeze/thaw treatment or extended benchtop time at room temperature compared to freshly processed QCs did not exceed $\pm 10\%$ (CV) and mean accuracies were within 98–117, respectively (Additional file 4).

Quantification of CAAPs in healthy humans and comparison between different whole blood-derived specimens. Using the current MRM-based method we were able to quantify concentrations at baseline levels from healthy donors (n = 6) for five out of nine CAAPs investigated (namely C36, C37, C40, C42 and C44; Fig. 1).

Absolute concentrations of C36, C37, C40, C42 and C44 in EDTA plasma were $0.105 \pm 0.030 \mu\text{M}$, $0.031 \pm 0.011 \mu\text{M}$, $0.017 \pm 0.001 \mu\text{M}$, $0.121 \pm 0.007 \mu\text{M}$ and $0.023 \pm 0.005 \mu\text{M}$, respectively (mean of $n = 6 \pm$ standard derivation). Since accuracy and precision of recovery rates in EDTA plasma exhibit best results among three tested blood-derived specimens, CAAP concentrations in lithium-heparin and serum were compared relative to EDTA plasma. Concentrations of CAAPs found in different matrices from same healthy donors revealed that the relative change of concentrations is consistent for serum compared to EDTA plasma (range of CV for five detected CAAPs: 2.5–8.7%; Fig. 1). However, mean serum concentrations differ between 94 and 131% compared to EDTA, depending on the respective CAAP. C36, C37 and C42 measured in lithium-heparin plasma also showed acceptable variation in relative concentrations compared to EDTA plasma (11.1%, 5.3% and 4% CV, respectively) and

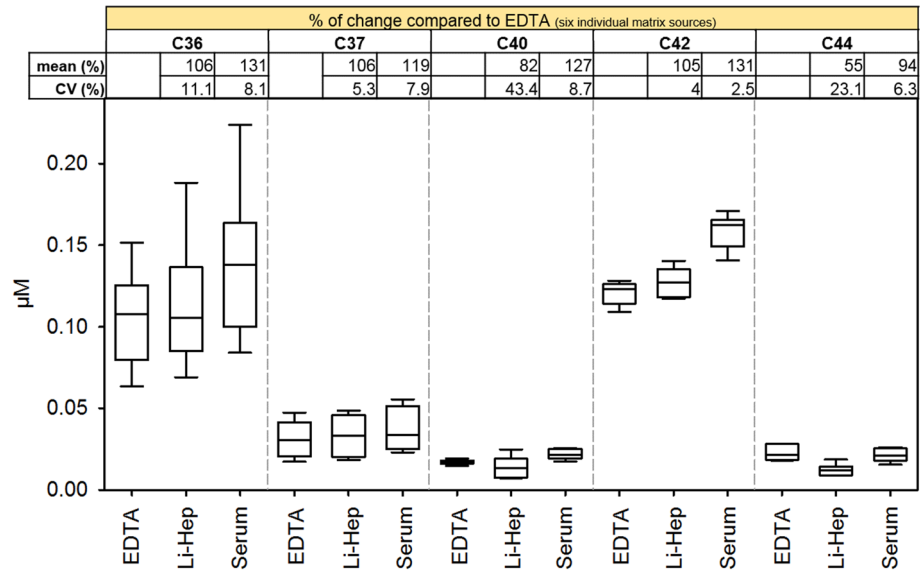


Figure 1. Comparison of CAAP levels in EDTA plasma, lithium-heparin plasma and serum. Relative changes (compared to EDTA plasma) were calculated for each donor individually (n=6) before mean accuracy (%) and CV (%) were calculated.

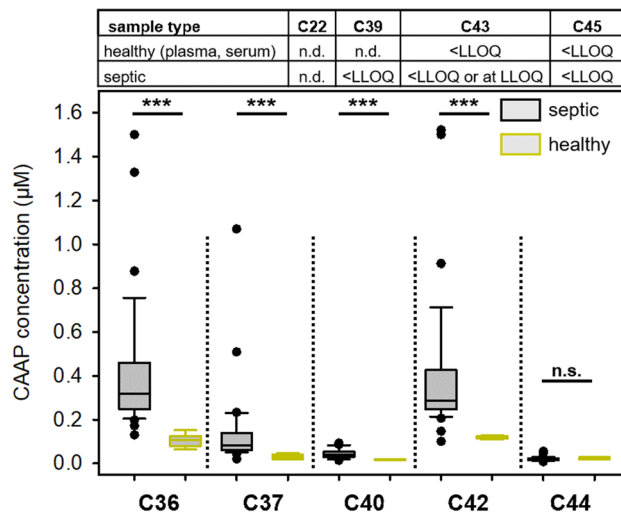


Figure 2. CAAPs abundance in healthy individuals (n=6) and septic patients (n=36, cohort A). Data are based on measurements of EDTA plasma samples, which were obtained from patients within the first three days after onset of sepsis. Statistical analysis was conducted using Mann–Whitney Rank Sum Test. *** $P < 0.001$, n.d. not detected, n.s. not significant.

comparable mean concentrations compared to EDTA (between 105 and 106%). However, C40 and C44 showed unacceptable high variations among individuals (43.4 and 23.1%) and mean concentrations were much lower in lithium-heparin plasma (82 and 55%) compared to EDTA.

Clinical applications. Since CAAPs can be generated from endogenous enzymatic activity associated with inflammation as well as by pathogens frequently causing septic shock, a clinical patient’s cohort suffering from sepsis was chosen to initially investigate CAAP profiles during infectious-induced systemic inflammation. EDTA plasma was used because it proved to be the most suitable blood-derived specimens during method validation. Concentrations of C36, C37, C40 and C42 were significantly higher in the sepsis cohort compared to healthy control samples ($P < 0.001$, respectively, Fig. 2). C44 in septic patient samples remains on healthy concentration level ($P = 0.229$). C22, C39, C43 and C45 were absent or below LLOQ.

CAAP	AUC [95% CI]	Cutoff ^a (μM)	Sensitivity (n ⁺ /n)	Specificity (n ⁻ /n)
C36	99% [98–101%]	0.162	97% (35/36)	100% (6/6)
C37	97% [92–102%]	0.048	97% (34/36)	71% (5/6)
C40	96% [91–102%]	0.020	88% (35/36)	50% (1/6)
C42	97% [92–103%]	0.137	97% (35/36)	100% (6/6)

Table 5. Accuracy of selected CAAPs for their potential to discriminate sepsis patients from healthy individuals. The data set used was the same as in Fig. 2. ^a Cutoffs are derived from Kolmogorov–Smirnov statistics. AUC: area under the receiver operating characteristics curve; CI: confidence interval; n⁺: measurements with positive test results; n⁻: measurements with negative test results; n: all measured values.

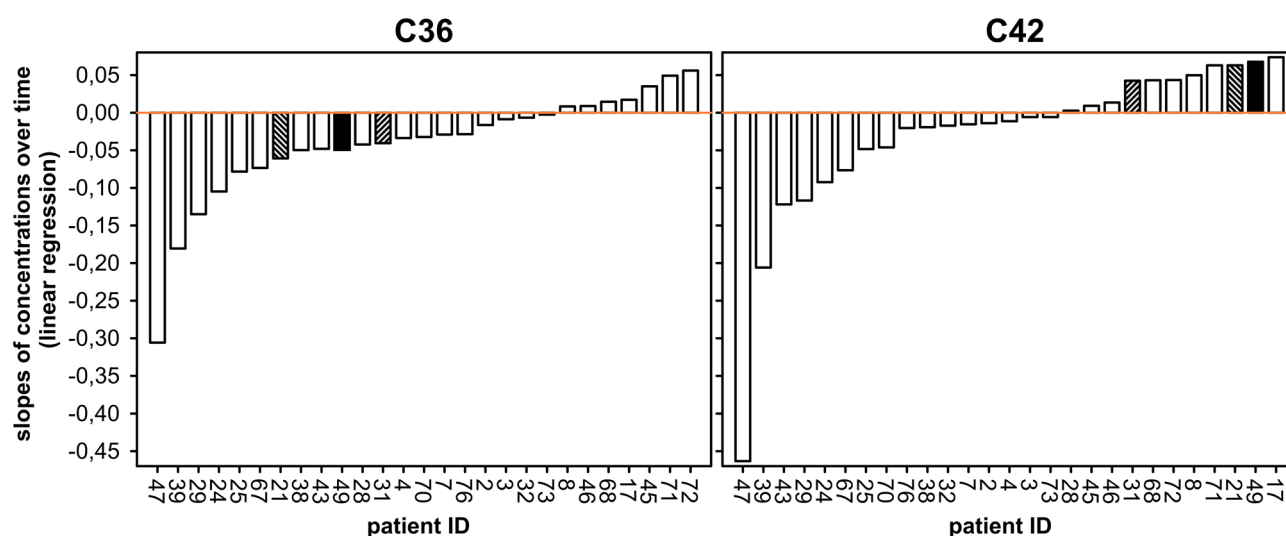


Figure 3. Development of C36 and C42 concentrations in septic patients. To obtain trends over time, linear regression analyses were conducted for patients with at least three samples collected during their stay at the ICU (cohort B, n = 27). Patients exhibiting opposite trends for C36 and C42 are highlighted.

Based on median values for each CAAP concentration, sepsis patients exhibit between 2.3 and 3.0 times higher concentrations of C36, C37, C40 and C42 than healthy individuals. Among the significantly increased CAAPs in sepsis samples compared to healthy individuals (Fig. 2), we have investigated the validity of C36, C37, C40 and C42 as potential biomarker for sepsis using ROC analysis (Table 5). C36 and C42 resulted in AUROC value of above 97% and high sensitivities (97%) and specificities (100%), respectively. Classifications of C37 and C40 were less sensitive and specific for discriminating sepsis from healthy patients.

For the two most abundant CAAPs C36 and C42, we have also analyzed their plasma concentrations in septic patients during the first week of treatment at the ICU (Fig. 3, n = 27).

Over the course of the disease, changes in concentrations of C36 and C42 vary greatly within the patient cohort; with C36 concentrations tending to decrease in the majority of cases (Fig. 3). We have further analyzed the development of C36 and C42 concentrations towards striking features among the sepsis cohort and we found that three out of 27 patients exhibit opposite trends for C36 and C42 concentrations over time (patient ID 21, 31 and 49; Fig. 3). For these three cases, C42 increases while C36 decreases over time.

Discussion

Since the role of CAAPs as biomarker has been proposed for many diseases^(36,38,39,42,46), see also Introduction), the proposed method is of important and broad clinical relevance. To this end, we also provide an overview about the current state of knowledge for CAAPs identified in vitro and in vivo (Table 6). In addition to CAAP generating conditions already described in the literature (Table 6), a vital role of CAAPs in other clinical contexts such as cancer progression^(18,45,56,57) and viral infections can be assumed due to increased MMP activities in the course of these diseases. For example, increased serum concentrations of neutrophil elastase (C36-generating enzyme) and MMP-12 (C42-generating enzyme) have been detected in severe COVID-19 patients⁽⁵⁸⁾. Biomarkers that allow to quantify systemic inflammation can become an essential tool for diagnosis as well as for monitoring the therapy of systemic inflammatory disorders, but are rarely available yet⁽⁵⁹⁾.

Due to the role of C42 as biomarker in systemic infection⁽⁴⁶⁾ and thus its potential application as sepsis biomarker in routine diagnostics, method development had focused on a rapid workflow. In contrast to the original LC–MS/MS method only targeting C42^{WT} and C42^{SNP46}, the current method possesses a rapid workflow and

CAAP ^a	in vivo (human)	in vitro human tissue/ cells	in vitro assays using purified enzymes		References
			Enzyme name	Enzyme host ^b	
C45 (G ³⁷³ A)	Not detected in plasma or serum of healthy or septic individuals				Current study
			Glycyl endopeptidase	<i>Carica papaya</i>	29,61
C44 (A ³⁷⁴ M)	Plasma & serum (no difference between healthy and septic individuals)				Current study
		Placenta			43,44
		BALF (higher concentrations in premature infants with bronchopulmonary dysplasia)			37
			MMP-11	human endogenous	6
		Adamalysin II	<i>Crotalus adamanteus</i>	29,62	
C43 (M ³⁷⁵ F)	Not detected in plasma or serum of healthy or septic individuals				Current study
			Thermolysin	<i>Bacillus thermoproteolyticus</i>	61
C42 (F ³⁷⁶ L)	Plasma & serum (higher concentrations in sepsis cohort than healthy individuals)				Current study
	EDTA plasma (higher concentrations in sepsis cohort than SIRS, HIV or neutropenia)				46
	NAF (only found in woman with breast cancer and among those only found in affected breast)				45
			MMP-1	Human endogenous	7,8
			MMP-7	Human endogenous	9–11
			MMP-8	Human endogenous	12–14
			MMP-9	Human endogenous	12,14
			MMP-12	Human endogenous	15,16
			MMP-13	Human endogenous	63
			MMP-25	Human endogenous	17
			MMP-26	Human endogenous	18,19
			Periodontain	<i>Porphyromonas gingivalis</i>	26,27
			Aureolysin	<i>Staphylococcus aureus</i>	27,28
		Thermolysin	<i>Bacillus thermoproteolyticus</i>	27,28,61	
		Papain	<i>Carica papaya</i>	29,61	
C40 (E ³⁷⁸ A)	Plasma & serum (higher concentrations in sepsis cohort than healthy individuals)				Current study
			Cathepsin L	Human endogenous	20
			Periodontain	<i>Porphyromonas gingivalis</i>	26,27
			Glutamyl endopeptidase	<i>Staphylococcus aureus</i>	28
			Aureolysin	<i>Staphylococcus aureus</i>	27
			Staphopain A	<i>Staphylococcus aureus</i>	27–29
		Pseudolysin	<i>Pseudomonas aeruginosa</i>	27	
C39 (A ³⁷⁹ I)	Not detected in plasma or serum of healthy or septic individuals				Current study
			Der p1 allergen	<i>Dermatophagoides pteronyssinus</i>	33
C37 (P ³⁸¹ M)	Plasma & serum (higher concentrations in sepsis cohort than healthy individuals)				Current study
			MMP-1	Human endogenous	8
			MMP-3	Human endogenous	7,10,21
			MMP-7	Human endogenous	10,11
			MMP-8	Human endogenous	13,14
			MMP-9	Human endogenous	14
			MMP-12 (mice)	Human endogenous	16
			MMP-13	Human endogenous	63
			MMP-25	Human endogenous	17
			MMP-26	Human endogenous	18,19
		Pseudolysin	<i>Pseudomonas aeruginosa</i>	27,30	

Continued

CAAP ^a	in vivo (human)	in vitro human tissue/ cells	in vitro assays using purified enzymes		References
			Enzyme name	Enzyme host ^b	
C36 (M ³⁸² S)	Plasma & serum (higher concentrations in sepsis cohort than healthy individuals)				Current study
	Spleen & bile (not found in plasma)				40
	BALF. Upregulated in patients with acute exacerbations idiopathic pulmonary fibrosis				38
	Gingival crevicular fluid (putative biomarker for GCF). Higher concentration than in healthy group				39
	Supernatants of activated (LPS-stimulated) neutrophils (not detected in unstimulated controls)				64
	Lung tissue (however, not correlated to COPD)				41
	Carotid artery tissue (symptomatic carotid artery stenosis undergoing carotid endarterectomy)				42
	BALF of premature infants				37
			Neutrophil Elastase	Human endogenous	5
			Cathepsin L	Human endogenous	20
			MMP-3	Human endogenous	10
			Prostate-specific antigen	Human endogenous	22,23
			Mesotrypsin (only Pittsburgh variant (M ³⁸² > R))	Human endogenous	24
			High temperature requirement A1	Human endogenous	25
			Serralysin	<i>Serratia marcescens</i>	27,31
			EspPa	enterohemorrhagic <i>Escherichia coli</i>	32
			Seaprose	<u><i>Aspergillus melleus</i></u>	34
			Endopeptidase (ragweed)	<u><i>Ambrosia artemisiifolia</i></u>	35
			Papain	<u><i>Carica papaya</i></u>	27,29,61
		Trypsin	<u><i>Streptomyces erythraeus</i></u>	65	
		bovines trypsin	bovine	65	
		porcine pancreatic elastase	porcine	66	
		α -chymotrypsin	bovine	61	
C22 (F ³⁹⁶ L)	Not detected in plasma or serum of healthy or septic individuals				Current study
	Urine (higher concentration in glomerular kidney disease patients compared to healthy)				36
	BALF (higher concentrations in premature infants with bronchopulmonary dysplasia)				37
			MMP-7	human endogenous	11

Table 6. Summary of known sources for CAAPs. ^ain brackets cleavage site numbering according to 418 amino acid sequence length of A1AT including precursor molecule of 24 amino acids⁶⁰ using one-letter-code for amino acids. ^bbold: human infectious microbes, underlined: not human infectious organism. A1AT: α 1-Antitrypsin; CAAP: C-terminal region of α 1-Antitrypsin; MMP: matrix metalloproteinase; BALF: bronchoalveolar lavage fluid. NAF: nipple aspiration fluids.

optimized chromatographic conditions for eighteen CAAP analytes. The entire process from sample preparation to quantitative results can be completed in less than one hour (30 min. sample preparation, 12 min. LC run). Working ranges were optimized based on results for carryover and specificity as well as concentrations detected in healthy and septic individuals. Concentration-dependent responses of all investigated CAAPs were linear across more than two orders of magnitude. Therefore, time-consuming steps for sample preparation (e.g. extraction or dilution), which are usually applied, are not necessary. In addition to the more efficient workflow, quantification of CAAPs in healthy individuals can now also be achieved (Fig. 1) due to increased sensitivity of the new method compared to the previous method⁴⁶. Finally, tests determining accuracy and precision (within-run repeatability and between-runs) of back-calculated CAAP concentrations using QC samples were successfully passed (Table 2).

Even though results of specificity between WT and SNP of some CAAPs are higher than 20% of the respective LLOQ (Additional file 2), we assume that the chance of incorrectly determined concentrations due to interferences from other CAAPs is negligible due to several reasons. First, concentrations below the LLOQ are generally not taken for final data analysis. Second, WT- and SNP-variant would both be considered in one sample in case of heterozygote genotype of rs1303 polymorphism which is true for only 37% of European American individuals⁶⁷. Third, among the analytes which exceed limits of specificity measures according to guidelines (maximum 20% of the LLOQ)^{54,55}, C36 is only one for which we have actually measured concentrations near the ULOQ. Fourth, back-calculated concentrations of WT and SNP which differ greater than 30% from each other are not considered as heterozygote genotype.

Combining results from recovery rates and absolute concentrations in healthy donors (Table 3, Fig. 1), EDTA plasma and serum are appropriate matrices to quantitatively measure CAAPs, whereas lithium-heparin plasma revealed results with high variations among individuals. Using lithium-heparin plasma for CAAP measurements is hence not suggested. Irrespective of the matrix, comparison of respective CAAP concentrations among different clinical entities (e.g. healthy versus diseased) should be performed within the same matrix, if possible.



Figure 4. Cleavage sites of selected CAAPs within the C-terminal amino acid sequence of A1AT. CAAPs are named after their respective amino acid lengths after cleavage. Yellow: 25 residue reactive centre loop of A1AT (UniProtKB). Red: single nucleotide polymorphism rs1303⁵³ in the CAAP sequence (E > D³⁷⁶).

Nevertheless, for data analysis it is recommended to define reference ranges for each CAAP concentration in each matrix.

The presence of C36, C37, C40, C42 and C44 in healthy individuals (Fig. 2) is in agreement with knowledge from the literature as those CAAPs have been reported to be generated endogenously in humans (Table 6). However, apart from our own previous study⁴⁶, this is to the best of our knowledge the first report about quantitatively measured C-terminal cleavage products of alpha-1-antitrypsin in blood-derived samples. Johansson and colleagues analyzed CAAPs in plasma, bile and spleen using liquid–liquid extraction and amino acid sequencing techniques⁴⁰. However, they have detected C36 in bile and spleen only but not in plasma. Four peptides (C22, C39, C43, C45) were not detected or below the LLOQ (Fig. 2). Their absence in plasma is partly in agreement with knowledge from the literature (Table 6). C39, C43, and C45 have indeed never been detected in vivo; and in vitro identifications of C43⁶¹ and C45^{29,61} have been correlated only to enzymes that are not associated with human diseases yet. C39, however, has only been found in vitro as potential cleavage product associated with allergic reactions³³ whereas C22 has been identified in vivo in urine³⁶ and BALF³⁷. In addition to the higher concentrations of C42⁴⁶ in septic patients compared to healthy individuals (Fig. 2) our results demonstrate that C36, C37 and C40 seem to play a crucial role in infectious-induced systemic inflammation as well and thus might also have the potential to serve as sepsis biomarkers in blood-derived samples. And indeed, the validity of C36 and C42 as sepsis biomarker was confirmed by their high sensitivities and specificities, respectively (Table 5). C36 experiences the greatest change among CAAPs measured in septic patients compared to concentrations measured in healthy individuals (n = 36, Fig. 2). This observation might be related to MMP activity since it has been shown that higher plasma levels of MMP-3 are associated with septic shock and mortality⁶⁸. C22, C39, C43 and C45 seem to play only a minor, if any, role during systemic inflammation because they were not detected or below the LLOQ in septic patients (Fig. 2). C36 and C42 concentrations of samples from septic patients (n = 27) change over time (Fig. 3) suggesting that enzymatic activities and/or elimination kinetics are related to the course of infectious-induced systemic inflammation. It is in agreement with knowledge from the literature that formations of C36 and C42 are mediated through distinct enzymatic activities, respectively (Table 6). Of note, for three patients (ID 21, 31 and 49) we detected clearly opposite trends for C36 (decrease) and C42 (increase) concentrations over time (Fig. 3). Decrease of C36 is followed by high initial C36 concentrations; moreover all three cases were affected by pneumonia (site of sepsis infection) with very high SOFA scores at admission (patient 21: 11; patient 31: 15; patient 49: 15). It is well known that increased activity of neutrophil elastase is involved in the pathogenesis of various lung diseases such as pneumonia (see reviews for example^{69,70}). C36 can be formed by neutrophil elastase⁵ and has already been found in vivo in lung-correlated tissues^{37,38,41}. Further investigation and studies are needed to uncover potential correlations of CAAPs with, for example, site of infection, organ failure or specific enzymatic activities.

Conclusion

Since the generation of CAAPs is multifaceted and they have been found in a variety of biomaterials and in response to a wide range of pathological changes, our method provides a useful clinical tool for many diseases. We are confident that the presented method can be easily adopted towards a variety of biological materials in order to specifically study CAAP levels at sites of generation such as placenta, BALF, bile or urine as well.

Material and methods

Selection of target compounds. The scientific literature search was conducted manually for known cleavage sites of A1AT. Among the variety of C-terminal peptides of A1AT (CAAPs) a panel of nine full-length CAAPs was selected (Fig. 4) according to their experimental evidence. Fragments that were only predicted as well as intermediate fragments in the C-terminal region of A1AT (such as VIRIP) were not collected.

Due to a minor allele frequency for the single nucleotide polymorphisms (SNP) of A1AT (rs1303, 28%) within the investigated C-terminal amino acid sequence, the final CAAP panel consists of eighteen analytes (wild type [WT] and SNP for each CAAP length). Authentic CAAPs and internal standards were obtained from sb-PEPTIDE (SmartBioscience SAS, Saint Egrève, FRANCE) as lyophilized peptides in aliquots. C22, C37 and C42 containing isotopic labelled lysine (¹³C¹⁵N) were used as internal standards (IS) for quantification (C22¹⁵, C37¹⁵, C42¹⁵).

Sample preparation. Lyophilized authentic peptide standards were dissolved and diluted in a 70 g/L Albumin (from human serum, lyophilized, ≥ 99%, Sigma-Aldrich) in PBS (Sigma-Aldrich, St. Louis, MO, USA) solution. Internal standards C37¹⁵ and C42¹⁵ were dissolved in Milli-Q water (Millipore, Brussels, Belgium) contain-

ing 0.1% (v/v) formic acid ($\geq 95\%$, Sigma-Aldrich) whereas C22^{IS} was only dissolved in ultrapure water. Mixtures of CAAPs used as calibration standards (calibrants) and quality control samples (QCs) were prepared as stock solution to a final concentration of 14 μM , respectively, (except C40^{SNP} which was 5 μM) with subsequent serial dilutions. Calibrants and QCs were obtained from separate serial dilutions. Internal standard solution was prepared by adding equal volumes of each IS yielding a final concentration of 0.8 μM , respectively. All samples used for method development and validation were prepared and stored in 0.5 mL Protein LoBind Tubes (Eppendorf AG, Hamburg, Germany) in aliquots at $-80\text{ }^\circ\text{C}$ until use.

For LC–MS/MS analyses, 10 μL of internal standard solution was added to 35 μL of calibrant, QC or study sample and gently mixed by pipetting. This mixture was then briefly centrifuged (10 s; 16,000 g; $+10\text{ }^\circ\text{C}$; model 5415R, Eppendorf AG) before 90 μL of cooled methanol ($\geq 99.9\%$, Carl Roth, Karlsruhe, Germany) was added and briefly vortexed subsequently. After centrifugation (10 min; 16,000 g; $10\text{ }^\circ\text{C}$) 100 μL of supernatant was transferred into 2 mL brown glass autosampler vials using 200 μL glass inserts (Wicom, Heppenheim, Germany).

LC–MS/MS analyses. For chromatographic separation, a Shimadzu HPLC system (Duisburg, Germany) was used which is equipped with a binary pump (LC20AB), a thermostatic autosampler (SIL20AC) and a thermostatic column compartment (CTO20AC). 5 μL sample was injected from the autosampler (maintained at $10\text{ }^\circ\text{C}$) and loaded on the UHPLC column (bioZen 3.6 μM Intact C4, $2.1 \times 100\text{ mm}$, Phenomenex, Aschaffenburg, Germany). The column oven was maintained at $45\text{ }^\circ\text{C}$; solvent A was 0.1% formic acid in ultrapure water (v/v) and solvent B was 0.1% formic acid in LC–MS Grade acetonitrile (v/v, $\geq 99.95\%$, Carl Roth). A step gradient was applied as follows: 5–25% B from 0–1 min., 25–46% B from 1–6 min., 46–85% B from 6–6.5 min., 85% B from 6.5–8.5 min., 85–5% B from 8.5–9.0 min. and 5% B from 9–12 min. The flow rate was 350 $\mu\text{L}/\text{min}$ from start to 6.5 min. and 10.6 to 12 min., respectively, and 600 $\mu\text{L}/\text{min}$ from 7.0 to 10.5 min.

For mass spectrometry detection, a Triple Quad 5500+ (AB SCIEX, Framingham, MA) in multiple reaction monitoring (MRM) scan type was used with Q1 at low and Q3 at unit resolution. The instrument was equipped with a Turbo V[™] ion source and operated in positive electrospray ionization mode with source parameters as follows: curtain gas = 35, collision gas = 8, ionSpray voltage = 5500, temperature = $700\text{ }^\circ\text{C}$, nebulization gas (GS1) = 70, drying gas (GS2) = 70.

Two transitions were monitored for each compound (quantifier, qualifier) and one for the internal standards using an intensity threshold of 50 cps. Corresponding compound-dependent parameters were optimized for each transition (Table 7) whereas entrance potential was 10 V for all transitions. Dwell time was 35 ms for all quantifier and 10 ms for all qualifier. A representative chromatogram is shown in Additional file 1.

Bioanalytical method validation. *Working range of calibrants* was defined based on CAAPs detected in samples from healthy donors (set to approximate lower limit of quantification) and in samples from septic patients (set to middle to high calibration range) which were re-analyzed from a previously work⁴⁶. Nine calibrants were used in total ranging from 0.01 μM to 1.5 μM thereby covering more than two orders of magnitude in concentration. *Linearity* was assessed determining mean linear regression coefficients of each calibration curve from 0.01 to 1.5 μM in eight independent analytical runs. However, respective LLOQs (lower limit of quantification) and ULOQs (upper limit of quantification) were defined individually based on natural occurrence (see above) and results from validation parameter directly affected individual working ranges (carry-over, specificity). Four QC samples were prepared and measured in total (QC1, QC2, QC3, and QC4) to cover the entire range of calibration. However, three QCs for each of the respective analytes were used for method validation. *Carry-over* was determined measuring pure albumin solutions prepared without internal standards (but equal amount and concentration of water/formic acid solution as regular internal standard solution, “blank albumin sample”) directly after the respective highest calibrants. Peak areas were compared to peak areas from respective LLOQ samples (prepared with regular internal standard solution). *Specificity* was assessed using single compounds at respective highest calibrant level which were prepared and calculated as described for carry-over. The specificity of analytes towards internal standards was determined using pure albumin solution with internal standard (“zero albumin sample”). *Accuracy and precision* was determined by back-calculated concentrations from repeated measurements of the same QC samples during one analytical run (*within-run repeatability*, $n=5$) and from freshly prepared samples during five independent analytical runs (*between-run*, $n=5$). Due to the unavailability of analyte-free biological matrix, *selectivity* of analytes were assessed in pure albumin solution containing internal standards. *Matrix effects* were determined calculating recovery rates and precision of each compound in human blood samples. Direct comparison between different anticoagulants (EDTA, lithium-heparin) and serum was performed using whole blood from the same human donor. Whole blood was collected in EDTA K₃, Lithium-Heparin Plasma-Gel and Serum Gel Z S-Monovettes (Sarstedt, Nümbrecht, Germany) from six healthy donors (3f./ 3 m; age from 27 to 45 years), respectively, and prepared using standard centrifugal conditions (10 min., 2762 g, room temperature; model 5804R, Eppendorf AG) before storage at $-80\text{ }^\circ\text{C}$. To minimize pre-analytical interferences, HIL indices (hemolysis, icterus, lipemia) were measured in lithium-heparin plasma as well as serum (Architect ci8200, Abbott Laboratories, Abbott Park, IL, USA) and results from both measures were valued as within normal ranges (data not shown). To determine *recovery rates in different blood matrices* spiked plasma was obtained by adding 5 μL of the spiking solution (peptide-mix standard in albumin: high [7 μM] and low [1 μM]) to 30 μL of different biological matrices from six healthy donors (EDTA plasma, lithium-heparin plasma and serum), respectively. Control samples (“0”) were pure albumin solutions added to biological matrices. Measurements were performed in duplicates. To determine recovery rates, accuracy was calculated by peak area ratios of analyte to internal standard using following equation: (area ratio of spiked sample) – (area ratio of endogenous concentration) / (area ratio of spiked albumin sample). To evaluate the consistency of matrix effect among individual donors, precision of peak area ratios of analyte to internal standard

Compound (mass ^a)		RT-window [min]	Precursor		Product [m/z]	DP [V]	CE [V]	CXP [V]	IS	
			m/z	charge						
C22 ^{WT} (2502.33)	Quantifier	3.3–3.5	626.8	[M + 4H] ⁴⁺	754.1	110	25	7	C22 ^{IS}	
	Qualifier		626.7		217.3	125	30	20		
C22 ^{SNP} (2488.32)	Quantifier	3.3–3.5	623.3	[M + 4H] ⁴⁺	749.4	110	25	7		
	Qualifier		623.3		217.3	125	30	20		
C36 ^{WT} (4132.23)	Quantifier	4.2–4.7	689.84	[M + 6H] ⁶⁺	787.8	105	20	6		C37 ^{IS}
	Qualifier		689.84		173.4	125	50	15		
C36 ^{SNP} (4118.21)	Quantifier	4.1–4.6	687.49	[M + 6H] ⁶⁺	785	105	20	6		
	Qualifier		687.49		173.4	125	20	15		
C37 ^{WT} (4263.27)	Quantifier	4.3–4.8	711.74	[M + 6H] ⁶⁺	787.8	105	30	6		
	Qualifier		854.09	[M + 5H] ⁵⁺	984.8	125	40	20		
C37 ^{SNP} (4249.25)	Quantifier	4.3–4.8	709.5	[M + 6H] ⁶⁺	785.1	105	30	6		
	Qualifier		851.26	[M + 5H] ⁵⁺	981.1	125	40	20		
C39 ^{WT} (4473.40)	Quantifier	4.4–5.0	747.06	[M + 6H] ⁶⁺	728.2	105	30	6		
	Qualifier		896.05	[M + 5H] ⁵⁺	984.5	125	40	15		
C39 ^{SNP} (4459.39)	Quantifier	4.3–4.9	744.63	[M + 6H] ⁶⁺	785.1	105	35	6		
	Qualifier		744.63		129.2	125	40	15		
C40 ^{WT} (4544.44)	Quantifier	4.4–5.0	758.25	[M + 6H] ⁶⁺	728.2	105	20	6	C42 ^{IS}	
	Qualifier		910.38	[M + 5H] ⁵⁺	873.6	125	30	20		
C40 ^{SNP} (4530.42)	Quantifier	4.3–4.9	756.45	[M + 6H] ⁶⁺	725.9	105	20	6		
	Qualifier		907.51	[M + 5H] ⁵⁺	870.8	125	30	10		
C42 ^{WT} (4786.57)	Quantifier	4.6–5.2	799.2	[M + 6H] ⁶⁺	873.6	105	25	6		
	Qualifier		958.6	[M + 5H] ⁵⁺	1091.9	125	40	20		
C42 ^{SNP} (4772.55)	Quantifier	4.5–5.1	796.75	[M + 6H] ⁶⁺	870.7	105	25	6		
	Qualifier		956	[M + 5H] ⁵⁺	1088.4	125	40	15		
C43 ^{WT} (4933.64)	Quantifier	4.9–5.5	823.65	[M + 6H] ⁶⁺	873.4	105	25	6		
	Qualifier		988.28	[M + 5H] ⁵⁺	1091.9	125	40	15		
C43 ^{SNP} (4919.62)	Quantifier	4.8–5.4	821.3	[M + 6H] ⁶⁺	870.8	105	25	6		
	Qualifier		985.4	[M + 5H] ⁵⁺	1088.2	120	40	15		
C44 ^{WT} (5064.68)	Quantifier	5.0–5.6	845.35	[M + 6H] ⁶⁺	873.9	105	35	6		
	Qualifier		1014.5	[M + 5H] ⁵⁺	1091.9	125	40	15		
C44 ^{SNP} (5050.66)	Quantifier	5.0–5.5	843.08	[M + 6H] ⁶⁺	870.7	100	35	6		
	Qualifier		1011.59	[M + 5H] ⁵⁺	1088.1	125	40	15		
C45 ^{WT} (5135.71)	Quantifier	5.1–5.7	857.59	[M + 6H] ⁶⁺	873.3	100	35	6		
	Qualifier		1028.58	[M + 5H] ⁵⁺	1091.9	125	40	15		
C45 ^{SNP} (5121.70)	Quantifier	5.1–5.6	855.19	[M + 6H] ⁶⁺	871.0	100	35	6		
	Qualifier		1025.85	[M + 5H] ⁵⁺	1088.1	120	40	15		
C22 ^{IS} (2516.37)	Quantifier	3.3–3.5	630.06	[M + 4H] ⁴⁺	756.4	110	25	7		-
	Qualifier		630.06	[M + 4H] ⁴⁺	224.4	125	30	20		
C37 ^{IS} (4277.30)	Quantifier	4.3–4.8	714.01	[M + 6H] ⁶⁺	790.6	105	30	6		
	Qualifier		856.76	[M + 5H] ⁵⁺	988.0	125	40	15		
C42 ^{IS} (4807.62)	Quantifier	4.7–5.2	802.72	[M + 6H] ⁶⁺	876.3	105	25	6		
	Qualifier		802.72	[M + 5H] ⁵⁺	1095.1	125	40	15		

Table 7. Compound-dependent parameters for the detection and quantification of CAAPs. ^a Theoretical monoisotopic mass (g/mol). DP = declustering potential, RT = retention time, CE = collision energy, CXP = collision cell exit potential, SNP = single nucleotide polymorphism, IS = internal standard.

was investigated for six individual donors in each of the biological matrix. To verify the *linear response* of CAAPs in different matrices, pool matrices consisting of equal volumes from each of the six donors was prepared and spiked with standard peptide mix (14 μM stock) before serial dilutions in the same pool matrix were conducted. Investigations of analyte *stabilities* were carried out using QC samples. Autosampler stability was determined by injecting each QC at the beginning of the run and 20 h later during six independent runs. The CV (%) of the back-calculated concentration (n = 2) was used to ensure autosampler stability. To determine stability of analytes after two cycles of freezing and thawing (“freeze/ thaw”) as well as after chilling for 60 min. at room temperature (“benchtop”) three QCs at two concentrations levels were used (QC2 and QC3), respectively. Samples were analyzed against freshly prepared QCs.

	Cohort A, n = 36	Cohort B, n = 27
Age, median (range)	66 (31–84)	66 (31–84)
Female, n (%)	14 (39)	8 (30)
28-day-survival, n (%)	27 (75)	22 (81)
SOFA at day of study admission ^a , median (25–75 percentile range)	10 (7–13)	10 (9–13)
Site of infection, n (%)		
Abdominal	16 (44.4)	9 (33.3)
Pneumonia	10 (27.8)	11 (40.7)
Soft tissue	–	2 (7.4)
Primary bacteremia	5 (13.9)	1 (3.7)
Endocarditis	3 (8.3)	3 (11.1)
Urogenital	2 (5.6)	1 (3.7)
Microbial-positive infection, n (%)		
Positive blood culture	9 (37.5)	5 (31)
Multiple microbial-positive	5 (20.8)	5 (31)
<i>S. aureus</i>	4 (16.7)	3 (18.8)
<i>E. coli</i>	5 (20.8)	4 (25)
<i>P. aeruginosa</i>	3 (12.5)	–
<i>Enterococci</i>	–	–
others	5 (20.8)	3 (18.8)

Table 8. Patient characteristics. Severe sepsis/ septic shock was diagnosed according to the ACCP/SCCM criteria⁷² and corresponds to the Sepsis-3 definition⁷³. Cohort A includes all patients of whom blood samples were available within three days after sepsis onset. Cohort B includes patients of whom blood samples were available at least three different days after sepsis onset and during their stay at the ICU. ^a When SOFA was not available at the day of study admission, SOFA was taken from the next day (n = 4).

Study cohort. To initially determine CAAP profiles in sepsis patients, a well-characterized set of study samples provided by the Department of Anesthesiology and Intensive Care Therapy (Jena University Hospital) was chosen⁷¹. All Patients were treated at the Intensive Care Unit (ICU) and blood samples were taken within 24 h after septic symptoms emerged and within the following seven days. For data analysis and interpretation of CAAPs profiles, two subgroups were selected (cohort A and cohort B). Above all, we were interested in CAAP profiles to investigate their potential as early biomarkers. Therefore, we grouped all patients of whom blood samples were available within three days after sepsis onset (cohort A). Next, we were interested in CAAPs development. To this end, we grouped all patients of whom blood samples were available at least three different days after sepsis onset and during their stay at the ICU (cohort B). Patient characteristics of the subgroups are listed in Table 8.

Data processing and statistical analysis. Analyst Software (version 1.6.2 and 1.7.1) was used for mass spectrometer data acquisition and processing. The raw data were imported into the quantification wizard tool, peak integration was reviewed individually and results were generated in relation to the respective internal standard. A $1/x^2$ weighted quadratic regression was used to calculate the concentrations of each of the eighteen compounds.

To calculate final concentrations for each of the nine CAAP lengths, concentrations of C42^{WT} and C42^{SNP} were used as reference compounds for determining individual phenotypes of rs1303 polymorphisms (homozygote WT, homozygote SNP or heterozygote). A tolerance of maximum 30% coefficient of variance was accepted between concentrations of C42^{WT} and C42^{SNP} for the heterozygote type.

Graphs and statistical analysis were performed using SigmaPlot 14.0. Measurements are presented as boxplots (median, 10/90th percentile) with error bars. For the classification of CAAPs as biomarkers, receiver operating characteristics analyses and cross tables were performed using SPSS statistics version 27 (IBM, New Armonk, NY).

Ethics approval and consent to participate. The study was approved by the Ethics Committee of Jena University Hospital (protocol numbers: 2018–1145-Material, 2018-1145_1-Material, 4619–11/15) and conducted in accordance with the Declaration of Helsinki. All participants (or their legal guardians) gave their written informed consent for analyses and data collection on a consent documentation form.

Availability of data and materials

The datasets used and/or analysed during the current study are available from the corresponding author on reasonable request.

Received: 29 November 2021; Accepted: 22 February 2022

Published online: 09 March 2022

References

- Janciauskiene, S. Conformational properties of serine proteinase inhibitors (serpins) confer multiple pathophysiological roles. *Biochim. Biophys. Acta* **1535**(3), 221–235 (2001).
- Mkaouar, H. *et al.* Serine protease inhibitors and human wellbeing interplay: new insights for old friends. *PeerJ* **7**, e7224 (2019).
- Janciauskiene, S. M. *et al.* The discovery of alpha1-antitrypsin and its role in health and disease. *Respir. Med.* **105**(8), 1129–1139 (2011).
- Oriano, M. *et al.* Protease-Antiprotease Imbalance in Bronchiectasis. *Int. J. Mol. Sci.* **22**(11), 15 (2021).
- Banda, M. J. *et al.* The inhibitory complex of human alpha 1-proteinase inhibitor and human leukocyte elastase is a neutrophil chemoattractant. *J. Exp. Med.* **167**(5), 1608–1615 (1988).
- Pei, D., Majmudar, G. & Weiss, S. J. Hydrolytic inactivation of a breast carcinoma cell-derived serpin by human stromelysin-3. *J. Biol. Chem.* **269**(41), 25849–25855 (1994).
- Mast, A. E. *et al.* Kinetics and physiologic relevance of the inactivation of alpha 1-proteinase inhibitor, alpha 1-antichymotrypsin, and antithrombin III by matrix metalloproteinases-1 (tissue collagenase), -2 (72-kDa gelatinase/type IV collagenase), and -3 (stromelysin). *J. Biol. Chem.* **266**(24), 15810–15816 (1991).
- Desrochers, P. E., Jeffrey, J. J. & Weiss, S. J. Interstitial collagenase (matrix metalloproteinase-1) expresses serpinase activity. *J. Clin. Invest.* **87**(6), 2258–2265 (1991).
- Sires, U. I. *et al.* Matrilysin is much more efficient than other matrix metalloproteinases in the proteolytic inactivation of alpha 1-antitrypsin. *Biochem. Biophys. Res. Commun.* **204**(2), 613–620 (1994).
- Zhang, Z. *et al.* Proteolysis of human native and oxidised alpha 1-proteinase inhibitor by matrilysin and stromelysin. *Biochim. Biophys. Acta* **1199**(2), 224–228 (1994).
- Kramer, H. B. *et al.* Elevation of intact and proteolytic fragments of acute phase proteins constitutes the earliest systemic antiviral response in HIV-1 infection. *PLoS Pathog.* **6**(5), e1000893 (2010).
- Vissers, M. C. *et al.* Cleavage and inactivation of alpha 1-antitrypsin by metalloproteinases released from neutrophils. *J. Clin. Invest.* **82**(2), 706–711 (1988).
- Knauper, V., Reinke, H. & Tschesche, H. Inactivation of human plasma alpha 1-proteinase inhibitor by human PMN leucocyte collagenase. *FEBS Lett.* **263**(2), 355–357 (1990).
- Desrochers, P. E. *et al.* Proteolytic inactivation of alpha 1-proteinase inhibitor and alpha 1-antichymotrypsin by oxidatively activated human neutrophil metalloproteinases. *J. Biol. Chem.* **267**(7), 5005–5012 (1992).
- Gronski, T. J. Jr. *et al.* Hydrolysis of a broad spectrum of extracellular matrix proteins by human macrophage elastase. *J. Biol. Chem.* **272**(18), 12189–12194 (1997).
- Banda, M. J. *et al.* Interaction of mouse macrophage elastase with native and oxidized human alpha 1-proteinase inhibitor. *J. Clin. Invest.* **79**(5), 1314–1317 (1987).
- Nie, J. & Pei, D. Rapid inactivation of alpha-1-proteinase inhibitor by neutrophil specific leukolysin/membrane-type matrix metalloproteinase 6. *Exp. Cell Res.* **296**(2), 145–150 (2004).
- Park, H. I. *et al.* Peptide substrate specificities and protein cleavage sites of human endometase/matrilysin-2/matrix metalloproteinase-26. *J. Biol. Chem.* **277**(38), 35168–35175 (2002).
- Li, W. *et al.* Matrix metalloproteinase-26 is associated with estrogen-dependent malignancies and targets alpha1-antitrypsin serpin. *Cancer Res.* **64**(23), 8657–8665 (2004).
- Johnson, D. A., Barrett, A. J. & Mason, R. W. Cathepsin L inactivates alpha 1-proteinase inhibitor by cleavage in the reactive site region. *J. Biol. Chem.* **261**(31), 14748–14751 (1986).
- Winyard, P. G. *et al.* Proteolytic inactivation of human alpha 1 antitrypsin by human stromelysin. *FEBS Lett.* **279**(1), 91–94 (1991).
- Zhang, W. M. *et al.* Prostate-specific antigen forms a complex with and cleaves alpha 1-protease inhibitor *in vitro*. *Prostate* **33**(2), 87–96 (1997).
- Zhang, W. M. *et al.* Characterization and determination of the complex between prostate-specific antigen and alpha(1)-protease inhibitor in benign and malignant prostatic diseases. *Scand. J. Clin. Lab. Invest.* **60**, 51–58 (2000).
- Szepessy, E. & Sahin-Toth, M. Human mesotrypsin exhibits restricted S1' subsite specificity with a strong preference for small polar side chains. *FEBS J* **273**(13), 2942–2954 (2006).
- Frochoux, V. *et al.* Alpha-1-antitrypsin: a novel human high temperature requirement protease A1 (HTRA1) substrate in human placental tissue. *PLoS ONE* **9**(10), e109483 (2014).
- Nelson, D. *et al.* Purification and characterization of a novel cysteine proteinase (periodontain) from *Porphyromonas gingivalis*. Evidence for a role in the inactivation of human alpha1-proteinase inhibitor. *J. Biol. Chem.* **274**(18), 12245–12251 (1999).
- Rapala-Kozik, M. *et al.* Comparative cleavage sites within the reactive-site loop of native and oxidized alpha1-proteinase inhibitor by selected bacterial proteinases. *Biol. Chem.* **380**(10), 1211–1216 (1999).
- Potempa, J., Watorek, W. & Travis, J. The inactivation of human plasma alpha 1-proteinase inhibitor by proteinases from *Staphylococcus aureus*. *J. Biol. Chem.* **261**(30), 14330–14334 (1986).
- Mast, A. E., Enghild, J. J. & Salvesen, G. Conformation of the reactive site loop of alpha 1-proteinase inhibitor probed by limited proteolysis. *Biochemistry* **31**(10), 2720–2728 (1992).
- Morihara, K. *et al.* Purification of human plasma alpha 1-proteinase inhibitor and its inactivation by *Pseudomonas aeruginosa* elastase. *J. Biochem.* **95**(3), 795–804 (1984).
- Virca, G. D. *et al.* Inactivation of human plasma alpha 1-proteinase inhibitor by a metalloproteinase from *Serratia marcescens*. *Biochim. Biophys. Acta* **704**(2), 267–271 (1982).
- Weiss, A., Joerss, H. & Brockmeyer, J. Structural and functional characterization of cleavage and inactivation of human serine protease inhibitors by the bacterial SPATE protease EspAlpha from enterohemorrhagic *E. coli*. *PLoS ONE* **9**(10), e111363 (2014).
- Kalsheker, N. A. *et al.* The house dust mite allergen *Der p1* catalytically inactivates alpha 1-antitrypsin by specific reactive centre loop cleavage: a mechanism that promotes airway inflammation and asthma. *Biochem. Biophys. Res. Commun.* **221**(1), 59–61 (1996).
- Korzus, E., Luisetti, M. & Travis, J. Interactions of alpha-1-antichymotrypsin, alpha-1-proteinase inhibitor, and alpha-2-macroglobulin with the fungal enzyme, seaprose. *Biol. Chem. Hoppe Seyler* **375**(5), 335–341 (1994).
- Bagarozzi, D. A. Jr. *et al.* Purification and characterization of a novel endopeptidase in ragweed (*Ambrosia artemisiifolia*) pollen. *J. Biol. Chem.* **271**(42), 26227–26232 (1996).
- Navarro-Munoz, M. *et al.* Uromodulin and alpha(1)-antitrypsin urinary peptide analysis to differentiate glomerular kidney diseases. *Kidney Blood Press. Res.* **35**(5), 314–325 (2012).
- Tirone, C. *et al.* Oxidative and proteolytic inactivation of alpha-1 antitrypsin in bronchopulmonary dysplasia pathogenesis: a top-down proteomic bronchoalveolar lavage fluid analysis. *Front. Pediatr.* **9**, 7 (2021).
- Carleo, A. *et al.* Proteomic characterization of idiopathic pulmonary fibrosis patients: stable versus acute exacerbation. *Monaldi Arch. Chest Dis.* <https://doi.org/10.4081/monaldi.2020.1231> (2020).

39. Preiano, M. *et al.* An analytical method for assessing optimal storage conditions of gingival crevicular fluid and disclosing a peptide biomarker signature of gingivitis by MALDI-TOF MS. *Proteomics Clin. Appl.* **12**(5), e1800005 (2018).
40. Johansson, J. *et al.* Identification of hydrophobic fragments of alpha 1-antitrypsin and C1 protease inhibitor in human bile, plasma and spleen. *FEBS Lett.* **299**(2), 146–148 (1992).
41. Subramaniam, D. *et al.* C-36 peptide, a degradation product of alpha 1-antitrypsin, modulates human monocyte activation through LPS signaling pathways. *Int. J. Biochem. Cell. Biol.* **38**(4), 563–575 (2006).
42. Dichtl, W. *et al.* The carboxyl-terminal fragment of alpha 1-antitrypsin is present in atherosclerotic plaques and regulates inflammatory transcription factors in primary human monocytes. *Mol. Cell. Biol. Res. Commun.* **4**(1), 50–61 (2000).
43. Niemann, M. A., Baggott, J. E. & Miller, E. J. Inhibition of human serine proteases by SPAAT, the C-terminal 44-residue peptide from alpha 1-antitrypsin. *Biochim. Biophys. Acta* **1340**(1), 123–130 (1997).
44. Niemann, M. A., Narkates, A. J. & Miller, E. J. Isolation and serine protease inhibitory activity of the 44-residue, C-terminal fragment of alpha 1-antitrypsin from human placenta. *Matrix* **12**(3), 233–241 (1992).
45. Zhou, J. *et al.* A unique proteolytic fragment of alpha 1-antitrypsin is elevated in ductal fluid of breast cancer patient. *Breast Cancer Res. Treat.* **123**(1), 73–86 (2010).
46. Blaurock, N. *et al.* C-terminal alpha-1 antitrypsin peptide: a new sepsis biomarker with immunomodulatory function. *Mediators Inflamm.* **2016**, 6129437 (2016).
47. Gogol, M. *et al.* Inactivation of alpha 1-proteinase inhibitor by *Candida albicans* aspartic proteases favors the epithelial and endothelial cell colonization in the presence of neutrophil extracellular traps. *Acta Biochim. Pol.* **63**(1), 167–175 (2016).
48. Banda, M. J. *et al.* Alpha 1-proteinase inhibitor is a neutrophil chemoattractant after proteolytic inactivation by macrophage elastase. *J. Biol. Chem.* **263**(9), 4481–4484 (1988).
49. Janciauskiene, S., Moraga, F. & Lindgren, S. C-terminal fragment of alpha 1-antitrypsin activates human monocytes to a pro-inflammatory state through interactions with the CD36 scavenger receptor and LDL receptor. *Atherosclerosis* **158**(1), 41–51 (2001).
50. Campbell, R. A. *et al.* Placental HTRA1 cleaves alpha-1-antitrypsin to generate a NET-Inhibitory Peptide. *Blood* **138**, 977–988 (2021).
51. Blaurock-Möller, N. *et al.* CAAP48, a new sepsis biomarker, induces hepatic dysfunction in an *in vitro* liver-on-chip model. *Front. Immunol.* **10**(273), 273 (2019).
52. Gerbod-Giannone, M. C. *et al.* Suppression of cholesterol 7alpha-hydroxylase transcription and bile acid synthesis by an alpha 1-antitrypsin peptide via interaction with alpha 1-fetoprotein transcription factor. *J. Biol. Chem.* **277**(45), 42973–42980 (2002).
53. Graham, A. *et al.* Characterisation of the alpha-1-antitrypsin M3 gene, a normal variant. *Hum. Genet.* **85**(3), 381–382 (1990).
54. Agency, E. M., *Guideline on bioanalytical method validation*. 2011, Committee for Medicinal Products for Human Use (CHMP).
55. Agency, E. M., draft: ICH guideline M10 on bioanalytical method validation (Step 2b). 2019.
56. Egeblad, M. & Werb, Z. New functions for the matrix metalloproteinases in cancer progression. *Nat. Rev. Cancer* **2**(3), 161–174 (2002).
57. Kataoka, H. *et al.* Enhanced tumor growth and invasiveness *in vivo* by a carboxyl-terminal fragment of alpha 1-proteinase inhibitor generated by matrix metalloproteinases: a possible modulatory role in natural killer cytotoxicity. *Am. J. Pathol.* **154**(2), 457–468 (1999).
58. Zerimech, F. *et al.* Protease-antiprotease imbalance in patients with severe COVID-19. *Clin. Chem. Lab. Med.* **59**(8), E330–E334 (2021).
59. Bauer, M. *et al.* A transcriptomic biomarker to quantify systemic inflammation in sepsis - a prospective multicenter phase II diagnostic study. *EBioMedicine* **6**, 114–125 (2016).
60. Long, G. L. *et al.* Complete sequence of the cDNA for human alpha 1-antitrypsin and the gene for the S variant. *Biochemistry* **23**(21), 4828–4837 (1984).
61. Chang, W. S. *et al.* Probing serpin reactive-loop conformations by proteolytic cleavage. *Biochem. J.* **314**, 647–653 (1996).
62. Kress, L. F. *et al.* Characterization of the inactive fragment resulting from limited proteolysis of human alpha-1-proteinase inhibitor by *Crotalus-adamanteus* proteinase-li. *J. Biol. Chem.* **254**(12), 5317–5320 (1979).
63. Wilkinson, D. J. *et al.* Matrix metalloproteinase-13 is fully activated by neutrophil elastase, and inactivates its serpin inhibitor, alpha-1 antitrypsin: Implications for osteoarthritis. *Febs j* **289**, 121–139 (2021).
64. Matamala, N. *et al.* Identification of novel short C-terminal transcripts of human SERPINA1 gene. *PLoS ONE* **12**(1), e0170533 (2017).
65. Vukoti, K. M., Kadiyala, C. S. & Miyagi, M. *Streptomyces erythraeus* trypsin inactivates alpha 1-antitrypsin. *FEBS Lett.* **585**(24), 3898–3902 (2011).
66. Ossanna, P. J. *et al.* Oxidative regulation of neutrophil elastase-alpha-1-proteinase inhibitor interactions. *J. Clin. Investig.* **77**(6), 1939–1951 (1986).
67. Exome Variant Server, NHLBI GO Exome Sequencing Project (ESP), Seattle, WA (<http://evs.gs.washington.edu/EVS/>) [accessed 2021 July].
68. Jones, T. K. *et al.* Elevated Plasma Levels of Matrix Metalloproteinase-3 and Tissue-Inhibitor of Matrix Metalloproteinases-1 Associate with Organ Dysfunction and Mortality in Sepsis. *Shock* **57**, 41–47 (2021).
69. Polverino, E. *et al.* The role of neutrophil elastase inhibitors in lung diseases. *Chest* **152**(2), 249–262 (2017).
70. Domon, H. & Terao, Y. The role of neutrophils and neutrophil elastase in pneumococcal pneumonia. *Front. Cell Infection Microbiol.* <https://doi.org/10.3389/fcimb.2021.615959> (2021).
71. Kramer, M. *et al.* Alternative splicing of SMPD1 in human sepsis. *PLoS ONE* **10**(4), e0124503 (2015).
72. Bone, R. C. *et al.* Definitions for sepsis and organ failure and guidelines for the use of innovative therapies in sepsis. The ACCP/SCCM Consensus Conference Committee. American College of Chest Physicians/Society of Critical Care Medicine. *Chest* **101**(6), 1644–1655 (1992).
73. Singer, M. *et al.* The third international consensus definitions for sepsis and septic shock (Sepsis-3). *Jama-J. Am. Med. Assoc.* **315**(8), 801–810 (2016).

Acknowledgements

The authors thank Kerstin Stein for her support in sample preparation. We are grateful to all the study participants for their valuable contribution.

Author contributions

A.B. design of the study; method development; acquisition, analyses and interpretation of the data; writing the manuscript. C.S.P. analyses, discussion, interpretation and critical reviewing of data; sepsis cohort: acquisition of study samples, patient inclusion, and survey of clinical data. C.S.C. initial involvement in the selection of peptides and albumin matrix. M.B. discussion, interpretation and critical reviewing of data; sepsis cohort: conception of the study and survey of clinical data. M.K. conception and design of the study; discussion, interpretation and critical reviewing of data. All authors contributed to the submitted version of the manuscript.

Competing interests

PD Dr. Dr. Kiehntopf and Dr. Bigalke are inventors of a patent covering the presented method as a tool for characterizing systemic inflammation (applicant: University Hospital Jena; inventors: Arite Bigalke and Michael Kiehntopf; application number: 22154836.5; status of application: submitted). The University Hospital Jena is also applicant of other published patents which are related to methods determining the origin of an infection (EP17719610.2; EP16167699.4). A patent covering the initial identification of C42 is published as well (published as CN104204808, EP2592421, EP2780719, US20170242035; Applicant: University Hospital Jena; Inventors: Michael Kiehntopf, Diana Schmerler, Thomas Deufel, Frank Brunkhorst). C. Schnabel, C. Sponholz and M. Bauer declare no potential competing interests.

Additional information

Supplementary Information The online version contains supplementary material available at <https://doi.org/10.1038/s41598-022-07752-w>.

Correspondence and requests for materials should be addressed to A.B. or M.K.

Reprints and permissions information is available at www.nature.com/reprints.

Publisher's note Springer Nature remains neutral with regard to jurisdictional claims in published maps and institutional affiliations.



Open Access This article is licensed under a Creative Commons Attribution 4.0 International License, which permits use, sharing, adaptation, distribution and reproduction in any medium or format, as long as you give appropriate credit to the original author(s) and the source, provide a link to the Creative Commons licence, and indicate if changes were made. The images or other third party material in this article are included in the article's Creative Commons licence, unless indicated otherwise in a credit line to the material. If material is not included in the article's Creative Commons licence and your intended use is not permitted by statutory regulation or exceeds the permitted use, you will need to obtain permission directly from the copyright holder. To view a copy of this licence, visit <http://creativecommons.org/licenses/by/4.0/>.

© The Author(s) 2022